



Pergamon

Ocean Engineering 27 (2000) 841–866

**OCEAN
ENGINEERING**

www.elsevier.com/locate/oceaneng

Water wave interaction with an array of bottom-mounted surface-piercing porous cylinders

A.N. Williams*, W. Li

Department of Civil and Environmental Engineering, University of Houston, Houston, TX 77204-4791, USA

Received 18 September 1998; accepted 3 December 1998

Abstract

The interaction of water waves with arrays of bottom-mounted, surface-piercing circular cylinders is investigated theoretically. The sidewall of each cylinder is porous and thin. Under the assumptions of potential flow and linear wave theory, a semi-analytical solution is obtained by an eigenfunction expansion approach first proposed for impermeable cylinders by Spring and Monkmeyer (1974), and later simplified by Linton and Evans (1990). Analytical expressions are developed for the wave motion in the exterior and all interior fluid regions. Numerical results are presented which illustrate the effects of various wave and structural parameters on the hydrodynamic loads and the diffracted wave field. It is found that the porosity of the structures may result in a significant reduction in both the hydrodynamic loads experienced by the cylinders and the associated wave runup. © 2000 Elsevier Science Ltd. All rights reserved.

Keywords: Wave diffraction; Hydrodynamics; Porous cylinders; Breakwaters

1. Introduction

Quantifying the hydrodynamic interactions between the members of an array of cylindrical structures is an important topic in ocean engineering. These interactions

* Corresponding author. Tel.: + 1-713-743-4269; fax: + 1-713-743-4260; e-mail: anwilliams@jetson.uh.edu

may result in hydrodynamic loads and wave runup on the individual structures that differ significantly from the loads and runup they would experience in isolation. An exact solution for the diffraction of linear water waves by arrays of bottom-mounted, surface-piercing, impermeable circular cylinders was first given by Spring and Monkmeyer (1974) using an eigenfunction expansion approach. Subsequently, Linton and Evans (1990) made a major simplification to the theory proposed by Spring and Monkmeyer (1974), which allowed the evaluation of near-field quantities such as loads and runup on the cylinders in a much more straightforward manner. Kagemoto and Yue (1986) have developed another solution that is formally exact within the context of the linear theory. They have shown how a general three-dimensional water-wave diffraction problem concerning a structure consisting of a number of separated elements can be solved exactly in terms of the diffraction characteristics of each of the individual elements.

In the case where the cylinder spacing is large relative to the incident wavelength, approximate techniques may reasonably be used to quantify the hydrodynamic interactions between the members of multi-column structures. A popular approach, based on the wide-spacing assumption is the so-called modified plane-wave approach first developed by McIver and Evans (1984), and later used in a number of applications by McIver (1984), Williams and Demirbilek (1988), Williams and Abul-Azm (1989), and Williams and Rangappa (1994). All of the above studies, however, assume that the cylinders are impermeable.

There have been several studies dealing with wave diffraction by thin-walled porous cylindrical structures. Wang and Ren (1994) studied wave interaction with a concentric surface-piercing two-cylinder system. Wave interaction with a semi-porous cylindrical breakwater protecting an impermeable circular cylinder was investigated by Darwiche et al. (1994). Williams and Li (1998) recently extended this analysis to deal with the case where the interior cylinder is mounted on a large storage tank.

In this paper, The hydrodynamics of arrays of bottom-mounted surface-piercing circular cylinders each with a porous side-wall is investigated theoretically. The porous side-wall is considered to be thin and there exists an enclosed fluid region inside each cylinder. Under the assumptions of linearized potential flow, analytical expressions are obtained for the wave motion in each of the flow regions based on the eigenfunction expansion approach originally given by Spring and Monkmeyer (1974), as simplified by Linton and Evans (1990). Semi-analytical expressions are obtained for the hydrodynamic loads and runup on each cylinder and for the free surface elevation in the vicinity of the array. Numerical results are presented which illustrated the effects of the various wave and structural parameters on these quantities. It is found that the porosity of the cylinders may have a significant influence on the diffracted wave field and hydrodynamic loads experienced by the structures.

2. Theoretical development

The geometry of the problem is shown in Fig. 1. An arbitrary array of N bottom-mounted, surface-piercing, thin-walled porous cylinders of radius a_j , $j = 1, 2, \dots, N$,

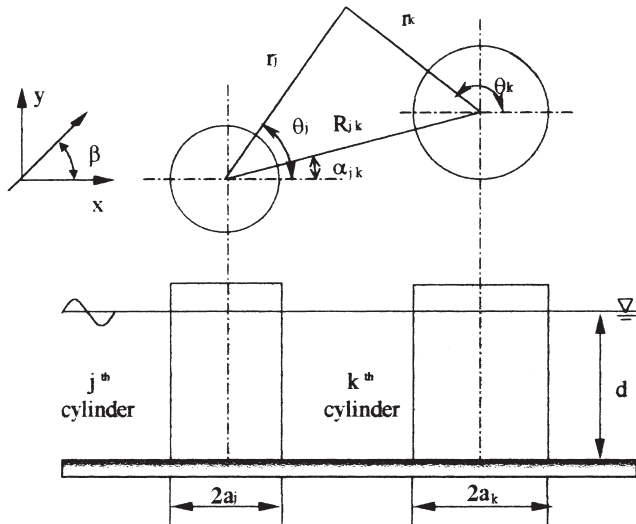


Fig. 1. Definition sketch for multiple porous cylinder diffraction problem.

is situated in water of uniform depth d . The global Cartesian coordinate system is defined with an origin located on the still-water level with the z -axis directed vertically upwards. The center of each cylinder, at $(x_j, y_j), j = 1, 2, \dots, N$, is taken as the origin of a local polar coordinate system (r_j, θ_j) , where θ_j is measured counterclockwise from the positive x -axis. The center of the k th cylinder has polar coordinates (R_{jk}, α_{jk}) relative to the j th cylinder, $j, k = 1, 2, \dots, N$. The coordinate relationship between the j th and k th cylinders is also shown in Fig. 1.

The array is subjected to a train of regular surface waves of height H and angular frequency ω propagating at an angle β to the positive x -axis. The small-amplitude, irrotational motion of the inviscid, incompressible fluid may be described in terms of velocity potential $\phi(x, y, z, t)$. The uniform geometry of the array members in the vertical allows the depth dependency in the solution to be factored out to give $\phi(x, y, z, t) = \text{Re}\{\Phi(x, y) f(z)e^{-i\omega t}\}$ where $\text{Re}\{\}$ denotes the real part of a complex expression, and

$$f(z) = -\frac{igH}{2\omega} \frac{\cosh k(z + d)}{\cosh kd} \tag{1}$$

In Eq. (1), g is the acceleration due to gravity and the wavenumber k is the positive real root of the dispersion relation $\omega^2 = gk \tanh kd$. The free-surface elevation is given by $\Xi(x, y, t) = \text{Re}\{\eta(x, y)e^{-i\omega t}\}$ where $\eta(x, y)$ is defined by

$$\eta(x, y) = \frac{H}{2} \Phi(x, y) \tag{2}$$

The fluid domain is divided into $N + 1$ regions: a single exterior region and N interior regions, defined by $0 \leq r_j \leq a_j, j = 1, 2, \dots, N$. The velocity potentials in

these regions will be denoted by $\Phi_1(x, y)$ and $\Phi_2^j(x, y), j = 1, 2, \dots, N$, respectively. It can be shown that these two-dimensional velocity potentials $\Phi(x, y)$ must satisfy a Helmholtz equation in each flow region, namely

$$\nabla^2 \Psi_j + k^2 \Psi_j = 0 \quad j = 0, 1, 2, \dots, N \tag{3}$$

where $\Psi_0 = \Phi_1(x, y)$ and $\Psi_j = \Phi_2^j(x, y), j = 1, 2, \dots, N$, as appropriate.

The boundary condition on the surface of cylinder j can be expressed as

$$\frac{\partial \Phi_1}{\partial r} = \frac{\partial \Phi_2^j}{\partial r} \quad \text{on } r_j = a_j \quad j = 1, 2, \dots, N \tag{4}$$

$$\frac{\partial \Phi_2^j}{\partial r} = W_j(\theta_j) \quad \text{on } r_j = a_j \quad j = 1, 2, \dots, N \tag{5}$$

where $W_j(\theta_j)$ is the spatial component of the normal velocity $w_j(\theta_j, z)$ of the fluid passing through the j th porous cylinder from the exterior region to the j th interior region, that is $w_j(\theta_j, z, t) = \text{Re}\{W_j(\theta_j) f(z) e^{-i\omega t}\}$ for $j = 1, 2, \dots, N$.

The wall of each cylinder is assumed to be thin with fine pores. The fluid flow passing through the porous walls is assumed to obey Darcy’s law. Hence, the porous flow velocity w is linearly proportional to the pressure difference across the thickness of the porous cylinder. Now the hydrodynamic pressure $p(x, y, z, t) = \text{Re}\{P(x, y) f(z) e^{-i\omega t}\}$ at any point in the fluid domain may be determined from the linearized Bernoulli equation as $P(x, y) = \rho i \omega \Phi(x, y)$ where ρ is the fluid density. Therefore it follows that

$$W_j(\theta_j) = \frac{\gamma}{\mu} \rho i \omega [\Phi_2^j - \Phi_1] \quad \text{on } r_j = a_j \quad j = 1, 2, \dots, N \tag{6}$$

where μ is the coefficient of dynamic viscosity and γ is a material constant having the dimension of length. Subsequently, the porosity of the breakwater will be characterized by the dimensionless parameter $G_0 = \rho \omega \gamma / (\mu k)$.

Finally, the diffracted component of the velocity potential in the exterior region must satisfy the usual radiation boundary condition, that is

$$\lim_{r \rightarrow \infty} \sqrt{r} \left[\frac{\partial}{\partial r} (\Phi_1 - \Phi_I) - ik(\Phi_1 - \Phi_I) \right] = 0 \tag{7}$$

where Φ_I is the spatial component of the incident wave potential, given by $\Phi_I = e^{ikr \cos(\theta - \beta)}$, where r is a global polar coordinate.

3. Analytical solutions

The incident plane wave potential can be expressed in the j th local polar coordinate system by

$$\Phi_1^j = I_j e^{ikr_j \cos(\theta_j - \beta)} \tag{8}$$

where $I_j = e^{ik(x_j \cos \beta + y_j \sin \beta)}$ is a phase factor associated with cylinder j . This in turn can be written as [see, for example, Abramowitz and Stegun (1972)]

$$\Phi_I^j = I_j \sum_{n=-\infty}^{n=\infty} J_n(kr_j) e^{in((\pi/2) - \beta + \theta_j)} \tag{9}$$

in which $J_n()$ denotes the Bessel function of the first kind of order n .

Following Linton and Evans (1990), the general form for the scattered wave emanating from cylinder j can be written as

$$\Phi_s^j = \sum_{n=-\infty}^{\infty} A_n^j Z_n^j H_n(kr_j) e^{in\theta_j} \tag{10}$$

for some set of complex numbers A_n^j . In Eq. (10), $Z_n^j = J_n'(ka_j)/H_n'(ka_j)$ where $H_n()$ is the Hankel function of the first kind of order n . The introduction of the factor Z_n^j simplifies the results that will eventually be obtained. The total potential in the exterior region can therefore be written as

$$\Phi_1 = \Phi_I + \sum_{j=1}^N \Phi_s^j = e^{ikr \cos(\theta - \beta)} + \sum_{j=1}^N \sum_{n=-\infty}^{\infty} A_n^j Z_n^j H_n(kr_j) e^{in\theta_j} \tag{11}$$

To account for interactions among the bodies, it is necessary to evaluate the scattered potential Φ_s^λ in terms of the representation of the incident potential Φ_I^λ at body j , $j = 1, 2, \dots, N, j \neq \lambda$. This can be accomplished by using Graf's addition theorem for Bessel functions (Abramowitz and Stegun, 1972) to give

$$H_n(kr_\lambda) e^{in(\theta_\lambda - \alpha_\lambda^j)} = \sum_{m=-\infty}^{\infty} H_{n+m}(kR_{\lambda_j}) J_m(kr_j) e^{im(\pi - \alpha_{\lambda_j} - \theta_j)} \tag{12}$$

for $\lambda, j = 1, 2, \dots, N, \lambda \neq j$. Eq. (12) is valid for $r_j < R_{\lambda_j}$, which is true on the boundary of the j th cylinder for all λ . The exterior region potential can be written as

$$\begin{aligned} \Phi_1^j(r_j, \theta_j) &= \sum_{n=-\infty}^{\infty} [I_j J_n(kr_j) e^{in((\pi/2) - \beta - \theta_j)} + A_n^j Z_n^j H_n(kr_j) e^{in\theta_j}] \tag{13} \\ &+ \sum_{\lambda=1, \lambda \neq j}^N \sum_{n=-\infty}^{\infty} A_n^\lambda Z_n^\lambda \sum_{m=-\infty}^{\infty} J_m(kr_j) H_{n+m}(kR_{\lambda_j}) e^{im(\pi - \theta_j + \alpha_\lambda^j) + in\alpha_\lambda^j} \end{aligned}$$

valid if $r_j < R_{\lambda_j}$ for all λ , i.e., this expansion is valid near cylinder j . The final term in Eq. (13) may be rearranged to give

$$\begin{aligned} \Phi_1^j(r_j, \theta_j) &= \sum_{n=-\infty}^{\infty} \{ [I_j e^{in(\pi/2 - \beta)} \\ &+ \sum_{\lambda=1, \lambda \neq j}^N \sum_{m=-\infty}^{\infty} A_m^\lambda Z_m^\lambda H_{m-n}(kR_{\lambda_j}) e^{i(m-n)\alpha_{\lambda_j}}] J_n(kr_j) \} \end{aligned}$$

$$+ A_n^j Z_n^j H_n(kr_j)\}e^{in\theta_j}. \tag{14}$$

The potential in the j th interior region, Φ_2^j , can be written as

$$\Phi_2^j = \sum_{n=-\infty}^{\infty} B_n^j J_n(kr_j)e^{in\theta_j} \tag{15}$$

for $j = 1, 2, \dots, N$, where the B_n^j are unknown potential coefficients. Applying boundary conditions, Eqs. (10) and (11), utilizing the orthogonality properties of eigenfunctions, leads to the following relationships between the potential coefficients A_n^j and B_n^j ,

$$I_j e^{in(\pi/2 - \beta)} + \sum_{\lambda=1, \lambda \neq j}^N \sum_{m=-\infty}^{\infty} A_m^\lambda Z_m^\lambda H_{m-n}^\lambda(kR_{\lambda j}) e^{i(m-n)\alpha_{\lambda j}} = B_n^j - A_n^j \tag{16}$$

$$\begin{aligned} & [I_j e^{in(\pi/2 - \beta)} + A_n^j Z_n^j H_n(ka_j) \\ & + \sum_{\lambda=1, \lambda \neq j}^N \sum_{m=-\infty}^{\infty} A_m^\lambda Z_m^\lambda H_{m-n}^\lambda(kR_{\lambda j}) e^{i(m-n)\alpha_{\lambda j}}] G_0 i = B_n^j [G_0 i J_n(ka_j) \\ & - J_n'(ka_j)] \end{aligned} \tag{17}$$

for $j = 1, 2, \dots, N, -\infty < n < +\infty$. Combining Eqs. (16) and (17), and using the Wronskian relationship for the Bessel functions results in the following infinite systems of equations,

$$\sum_{\lambda=1, \lambda \neq j}^N \sum_{m=-\infty}^{\infty} A_m^\lambda Z_m^\lambda H_{m-n}^\lambda(kR_{\lambda j}) e^{i(m-n)\alpha_{\lambda j}} + I_j e^{in(\pi/2 - \beta)} = \tag{18}$$

$$\begin{aligned} & - \left[\frac{2G_0}{\pi ka_j H_n(ka_j) J_n'(ka_j)} + 1 \right] A_n^j \\ B_n^j = & - \frac{2G_0}{\pi ka_j} \frac{A_n^j}{H_n'(ka_j) J_n(ka_j)} \end{aligned} \tag{19}$$

for $j = 1, 2, \dots, N, -\infty < n < +\infty$. Taking Eq. (18) into Eq. (14) gives the following simple form for $\Phi_1(r_j, \theta_j)$,

$$\Phi_1^j(r_j, \theta_j) = \sum_{n=-\infty}^{\infty} A_n^j \left[- \frac{2G_0 J_n(kr_j)}{\pi ka_j H_n'(ka_j) J_n'(ka_j)} - J_n(kr_j) + Z_n^j H_n(kr_j) \right] e^{in\theta_j} \tag{20}$$

valid for $r_j < R_{\lambda j}, \lambda = 1, 2, \dots, N$. In particular, taking $r_j = a_j$ and applying the Wronskian relationships for the Bessel functions to this Eq. (30), gives the exterior region velocity potential on the j th cylinder. This quantity is useful in calculating the force, moment and run-up on the j th cylinder, and is given by

$$\Phi_1^j(a_j, \theta_j) = \sum_{n=-\infty}^{\infty} \frac{-2A_n^j}{k\pi a_j H_n'(ka_j)} \left[i + \frac{G_0 J_n(ka_j)}{J_n'(ka_j)} \right] e^{in\theta_j} \tag{21}$$

for $j = 1, 2, \dots, N$. In order to calculate the potential coefficients A_n^j the infinite system in Eq. (18) is truncated to a $(2M + 1)N$ system of equations in $(2M + 1)N$ unknowns, i.e.,

$$\sum_{\lambda = 1, \lambda \neq j}^N \sum_{m = -M}^M A_m^\lambda Z_m^\lambda H_{m-n}^\lambda(kR_{\lambda j}) e^{i(m-n)\alpha_{\lambda j}} + I_j e^{in(\pi/2 - \beta)} = - \left[\frac{2G_0}{\pi k a_j H'_n(k a_j) J'_n(k a_j)} + 1 \right] A_n^j \tag{22}$$

for $j = 1, 2, \dots, N, n = -M, \dots, M$. This system may be solved by standard matrix techniques. The potential coefficients B_n^j may then be obtained from Eq. (19). In this manner the velocity potentials in each fluid region may be determined.

The solution to a number of limiting cases may be obtained from Eq. (22). If the porosity parameter $G_0 = 0$ (which corresponds to an impermeable cylinder), the linear system in Eq. (22) becomes

$$\sum_{\lambda = 1, \lambda \neq j}^N \sum_{m = -M}^M A_m^\lambda Z_m^\lambda H_{m-n}^\lambda(kR_{\lambda j}) e^{i(m-n)\alpha_{\lambda j}} + A_n^j = - I_j e^{in(\pi/2 - \beta)} \tag{23}$$

for $j = 1, 2, \dots, N, n = -M, \dots, M$, which recovers the result of Linton and Evans (1990).

Also, taking $N = 1$ in Eq. (22) and assuming that the cylinder center is located at the origin, then for $\beta = 0$,

$$A_n^1 = - \frac{e^{in(\pi/2)} H'_n(k a_1) J'_n(k a_1)}{\frac{2G_0}{\pi k a_1} + H'_n(k a_1) J'_n(k a_1)} \tag{24a}$$

$$B_n^1 = \frac{e^{in(\pi/2)} \frac{2G_0}{\pi k a_1}}{\frac{2G_0}{\pi k a_1} + H'_n(k a_1) J'_n(k a_1)} \tag{24b}$$

for $n = -M, \dots, M$. Eq. (24a) and (24b) recover the limiting case of wave interaction with a hollow porous cylinder reported by Wang and Ren (1994).

Finally if $G_0 = 0$ and $N = 1$, and again assuming that the cylinder center is located at the origin, then for $\beta = 0$,

$$A_n^1 = - i^n \tag{25}$$

which recovers the result of MacCamy and Fuchs (1954).

Returning to the multiple porous cylinder case, various quantities of engineering interest may now be computed. The exciting forces on an individual cylinder in the two orthogonal directions in the horizontal plane, F_x^j and F_y^j are obtained by the integration of the pressure on the surface of the cylinder, namely

$$\begin{bmatrix} F_x^j \\ F_y^j \end{bmatrix} = -\frac{\rho g H a_j}{2k} \tanh kd \int_0^{2\pi} [\Phi_1^i(a_j, \theta_j) - \Phi_2^i(a_j)] \begin{bmatrix} \cos \theta_j \\ \sin \theta_j \end{bmatrix} d\theta_j \tag{26}$$

Simplifying algebraically leads to the following result,

$$\begin{bmatrix} F_x^j \\ F_y^j \end{bmatrix} = -\begin{bmatrix} i \\ 1 \end{bmatrix} \frac{\rho g H}{k^2 H_1(ka_j)} \tanh kd \begin{bmatrix} A_{-1}^i - A_1^i \\ A_{-1}^i + A_1^i \end{bmatrix} \tag{27}$$

Similarly, the exciting moments on *j*th cylinder about the *x* and *y* axes about point (*x_j*, *y_j*, 0) can be written as

$$\begin{bmatrix} M_y^j \\ M_x^j \end{bmatrix} = \begin{bmatrix} i \\ -1 \end{bmatrix} \frac{\rho g H}{k^3 H_1(ka_j)} \frac{\cosh kd - 1}{\cosh kd} \begin{bmatrix} A_{-1}^i - A_1^i \\ A_{-1}^i + A_1^i \end{bmatrix} \tag{28}$$

For bottom-mounted, surface-piercing cylinders, the moments can be expressed in terms of the force components, namely

$$\begin{bmatrix} M_y^j \\ M_x^j \end{bmatrix} = \frac{\cosh kd - 1}{k \sinh kd} \begin{bmatrix} -F_x \\ F_y \end{bmatrix} \tag{29}$$

and so in the discussion of the numerical results, attention will be focussed on forces only.

The amplitude of the free surface is given in terms of the velocity potential by

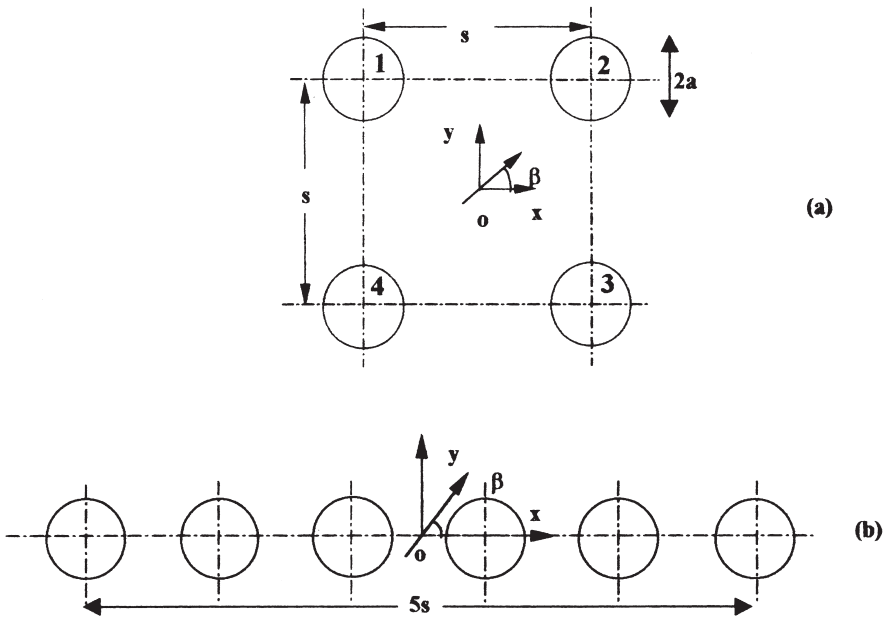


Fig. 2. Definition sketches for (a) four-cylinder array and (b) six-cylinder array.

Eq. (2). Eq. (20) provides an efficient method for the evaluation of free-surface amplitudes near a particular cylinder, while Eq. (21) allows for the efficient calculation of the wave runup on the outer surface of the j th cylinder, that is

$$|\eta(x,y)| = \frac{H}{2} \left| e^{ikr\cos(\theta - \beta)} + \sum_{j=1}^N \sum_{n=-\infty}^{\infty} A_n^j Z_n^j H_n(kr_j) e^{in\theta_j} \right| \tag{30}$$

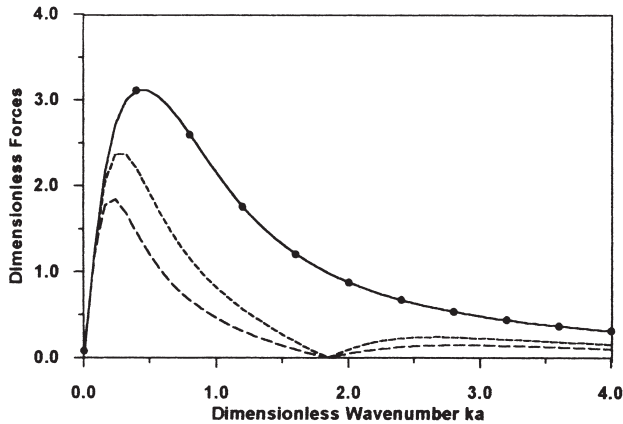


Fig. 3. Dimensionless hydrodynamic forces on a single circular cylinder for $d/a = 5$. Notations: — $G_0 = 0$; - - - $G_0 = 1$; - · - $G_0 = 2$. The symbols show the results of MacCamy and Fuchs (1954).

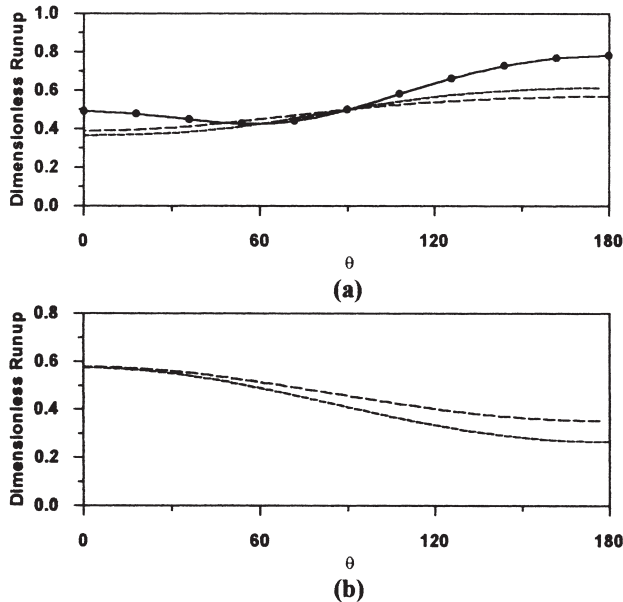


Fig. 4. Run-up profiles on the outer (a) and inner (b) walls of a single circular cylinder for $ka = 6$. Notations: — $G_0 = 0$; - - - $G_0 = 1$; - · - $G_0 = 2$. The symbols show the results of MacCamy and Fuchs (1954).

and

$$|\eta_i^j(a_j, \theta_j)| = \frac{H}{2} \left| \sum_{n=-\infty}^{\infty} \frac{-2A_n^j}{k\pi a_j H_n'(ka_j)} \left[i + \frac{G_0 J_n(ka_j)}{J_n'(ka_j)} \right] e^{in\theta_j} \right| \quad (31)$$

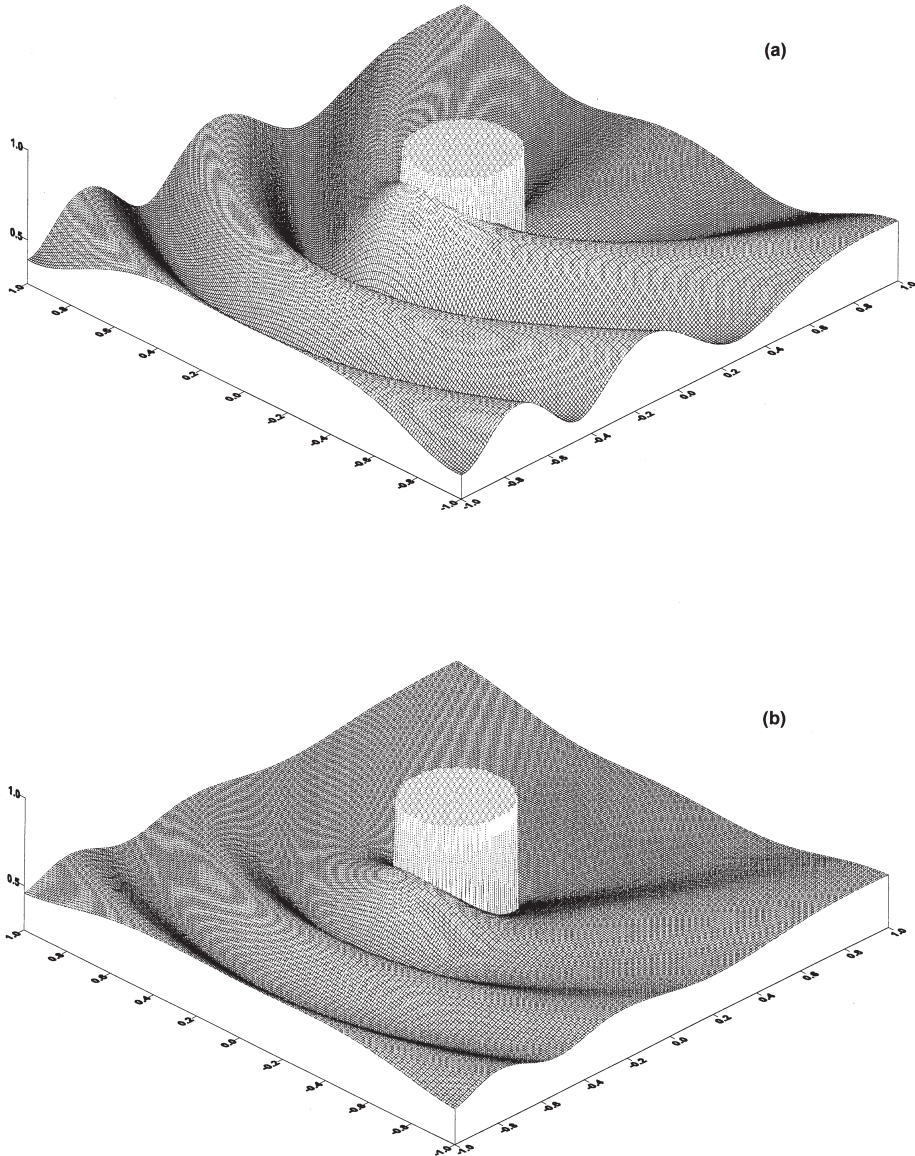


Fig. 5. Free-surface elevation in the vicinity of a single circular cylinder for $d/a = 5$, $ka = \pi/2$. Notations: (a) $G_0 = 0$; (b) $G_0 = 1$.

Finally, for the j th interior region, the free-surface amplitude and run-up may be calculated from the following equations,

$$|\eta_2^j(r_j, \theta_j)| = \frac{H}{2} \left| \sum_{n=-\infty}^{\infty} B_n^j J_n(kr_j) e^{in\theta_j} \right| \tag{32}$$

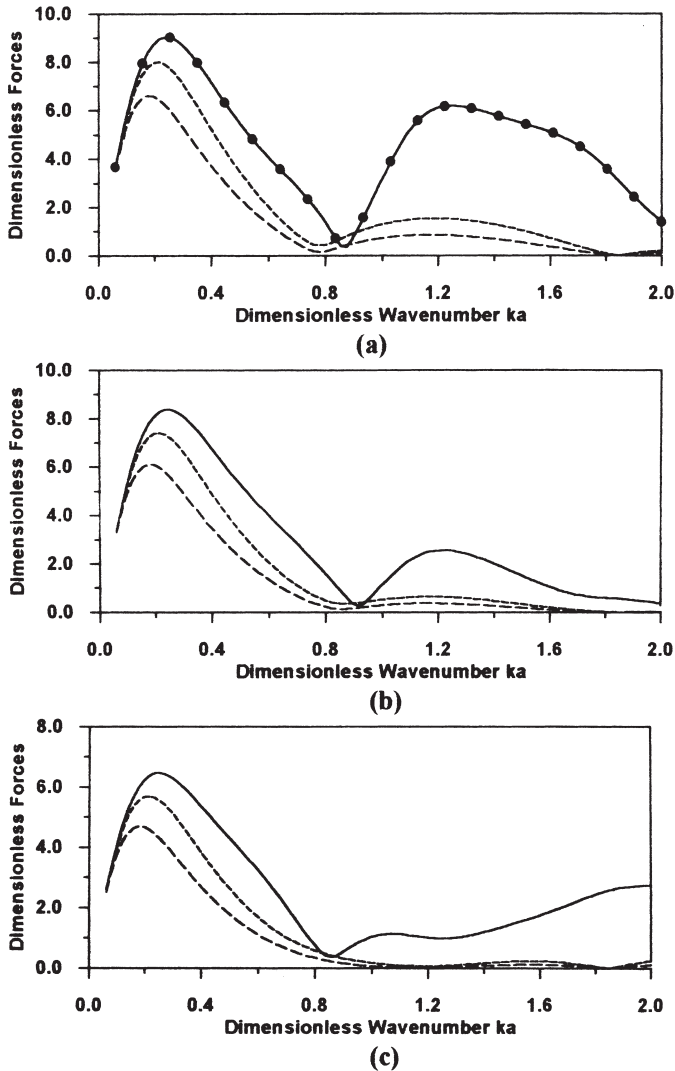


Fig. 6. Dimensionless hydrodynamic force in x -direction on a four-cylinder array with $d/a = 5$, $s/a = 4$ for (a) $\beta = 0^\circ$; (b) $\beta = 22.5^\circ$; (c) $\beta = 45^\circ$. Notations: — $G_0 = 0$; - - - $G_0 = 1$; - · - · $G_0 = 2$. The symbols in (a) are the results of Chakrabarti (1987).

$$|\eta_2^i(a_j, \theta_j)| = \frac{H}{2} \left| \sum_{n=-\infty}^{\infty} B_n^i J_n(ka_j) e^{in\theta_j} \right| \tag{33}$$

4. Numerical results and discussions

A computer program has been written to implement the above analysis, and the diffraction characteristics of several configurations have been studied. It is found

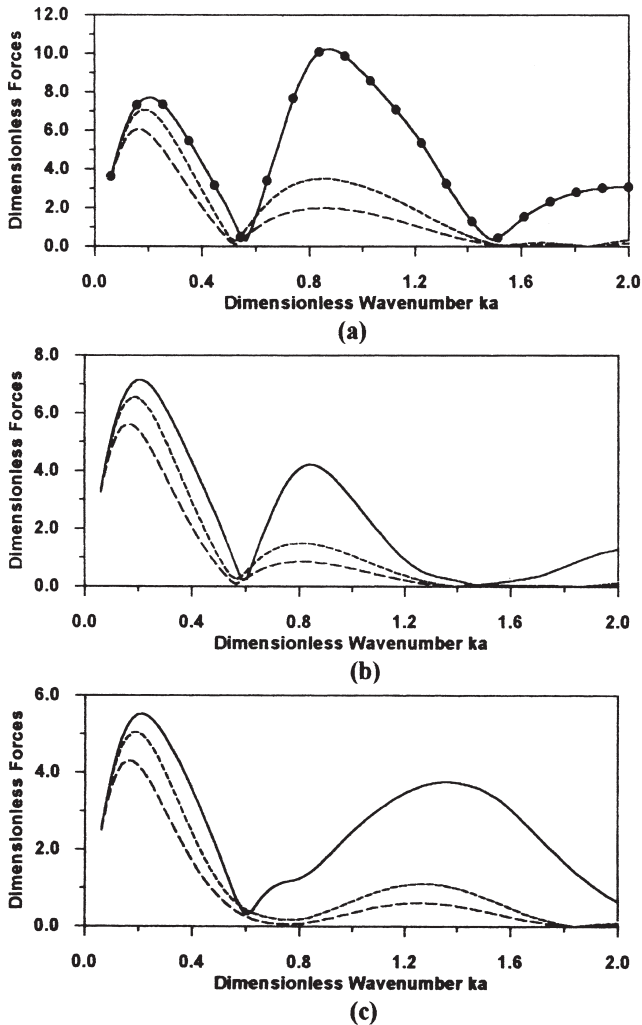


Fig. 7. Dimensionless hydrodynamic force in x -direction on a four-cylinder array with $d/a = 5$, $s/a = 6$ for (a) $\beta = 0^\circ$; (b) $\beta = 22.5^\circ$; (c) $\beta = 45^\circ$. Notations: — $G_0 = 0$; --- $G_0 = 1$; - · - $G_0 = 2$. The symbols in (a) are the results of Chakrabarti (1987).

that taking $M = 10$ in Eq. (22) for the all calculations appearing herein provides sufficient accuracy for engineering applications (1–2%). The correctness of the present theory and the associated computer program is verified through several limiting solutions appearing in the open literature. The following example configurations will be considered: an isolated cylinder; a structure possessing four columns of equal diameter in a configuration similar to large four-column platform [see Fig. 2(a)]; and, a breakwater system with six identical equally-spaced columns located in a straight line [see Fig. 2(b)]. In all figures, the forces are nondimensionalized by

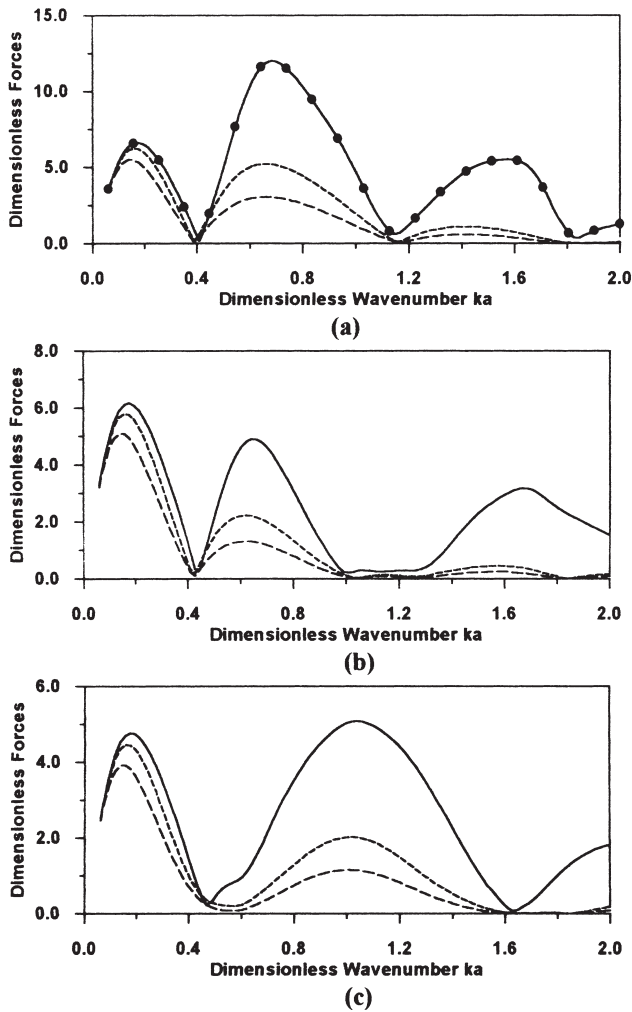


Fig. 8. Dimensionless hydrodynamic force in x -direction on a four-cylinder array with $d/a = 5$, $s/a = 8$ for (a) $\beta = 0^\circ$; (b) $\beta = 22.5^\circ$; (c) $\beta = 45^\circ$. Notations: — $G_0 = 0$; --- $G_0 = 1$; - - - $G_0 = 2$. The symbols in (a) are the results of Chakrabarti (1987).

$\rho g H \pi a^2$ and the magnitudes of free-surface elevations and runup are nondimensionalized by H .

Fig. 3 presents the results for the dimensionless wave forces for the isolated cylinder with $d/a = 5$ and $G_0 = 0, 1, 2$. For $G_0 = 0$, it is noted that the results of MacCamy and Fuchs (1954) are recovered. It can be seen that the force on the column can be reduced significantly by the porosity and the forces tend to decrease as the porosity parameter G_0 increases. Fig. 4 shows the runup amplitude both inside and outside the column for $ka = 0.6$. In Fig. 4(a) the results of MacCamy and Fuchs (1954) are again recovered. It can be seen, as expected, that the maximum runup

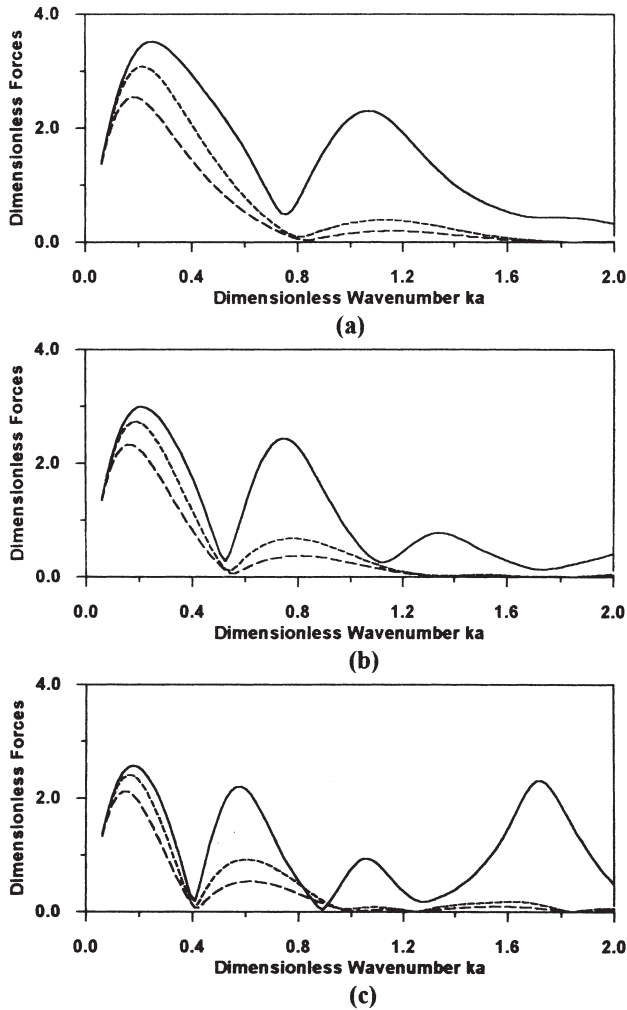


Fig. 9. Dimensionless hydrodynamic force in y-direction on a four-cylinder array with $d/a = 5$, $\beta = 22.5^\circ$, for (a) $s/a = 4$; (b) $s/a = 6$; (c) $s/a = 8$. Notations: — $G_0 = 0$; - - - $G_0 = 1$; - · - · $G_0 = 2$.

occurs at $\theta = 180^\circ$ and as G_0 increases, the maximum runup tends to decrease. It can be seen from Fig. 4(b) that the maximum run-up inside the column occurs at $\theta = 0^\circ$ and the magnitude of this maximum run-up increases as the porosity parameter G_0 increases. Fig. 5 presents the magnitude of the free surface elevation in the vicinity of single cylinder with $d/a = 5$, $ka = \pi/2$ and for a porosity parameter $G_0 = 0$

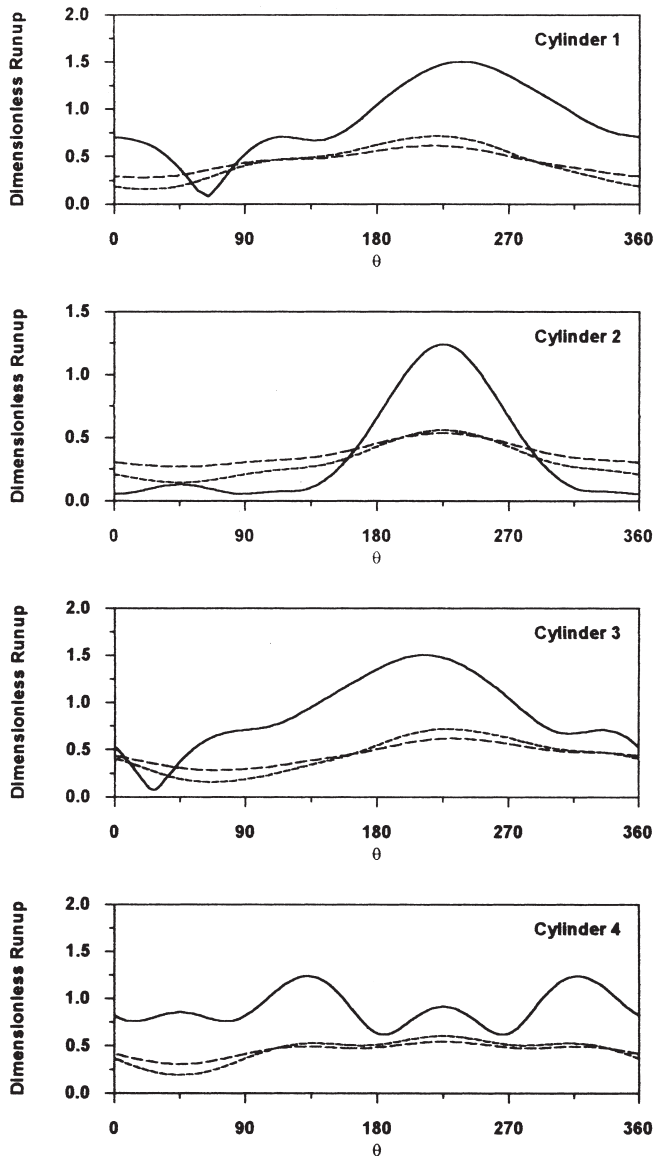


Fig. 10. Dimensionless run-up on outer wall of each cylinder of four-cylinder array for $s/a = 4$, $\beta = 45^\circ$ and $ka = \pi/2$. Notations: — $G_0 = 0$; - - - $G_0 = 1$; - · - · $G_0 = 2$.

and 1. The diffraction of the incident wave field by the column is clearly shown. It also shows that the porosity of the column decreases the diffracted wave field.

A four-cylinder array is now considered. The origin of the global coordinate system is at the geometric center of the array and the cylinders are numbered according to Fig. 2(a). Results are again presented for $d/a = 5$. The total forces in the x -direction are shown in Figs. 6–8 for a relative cylinder spacing $s/a = 4, 6, \text{ and } 8$, incident wave angles $\beta = 0^\circ, 22.5^\circ \text{ and } 45^\circ$, and porosity parameter $G_0 = 0, 1, 2$. The symbols in these figures represent the results of Chakrabarti (1987) for an array

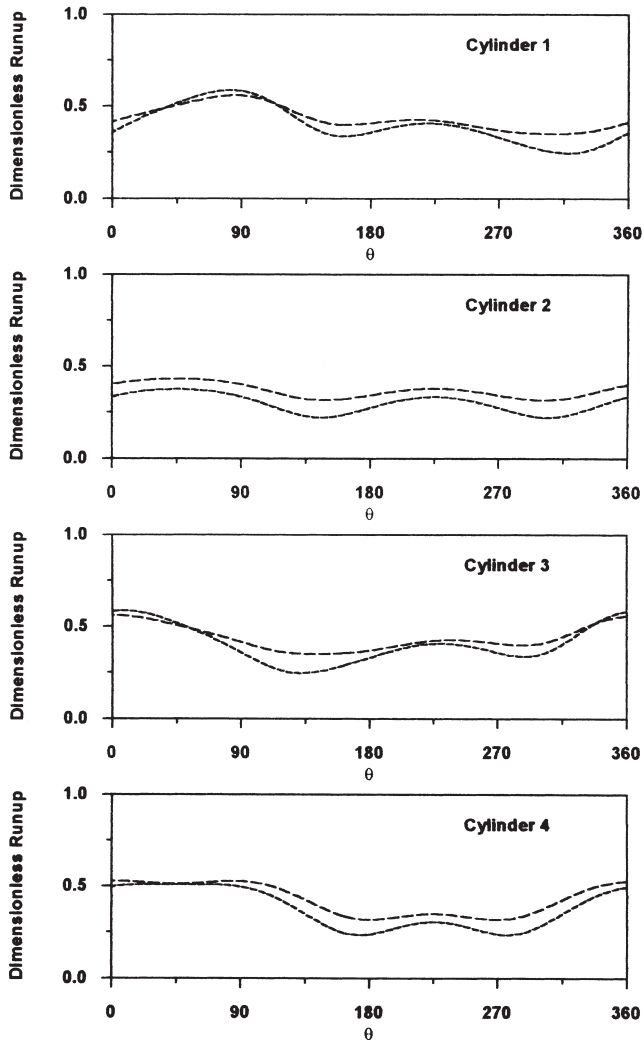


Fig. 11. Dimensionless run-up on inner wall of each cylinder of four-cylinder array for $s/a = 4$, $\beta = 45^\circ$ and $ka = \pi/2$. Notations: — $G_0 = 0$; - - - $G_0 = 1$; - · - · $G_0 = 2$.

of impermeable cylinders. The total forces in y -direction for $\beta = 22.5^\circ$ are shown in Fig. 9. For the other angles of wave incidence the forces in y -direction are either zero or may be inferred from symmetry. Generally speaking, the total loading on the four cylinder array can be reduced significantly by the cylinders' porosity. As an example of the influence of porosity on runup for this array configuration, Figs. 10–13 present the run-up on each cylinder for a cylinder spacing to radius ratio s/a

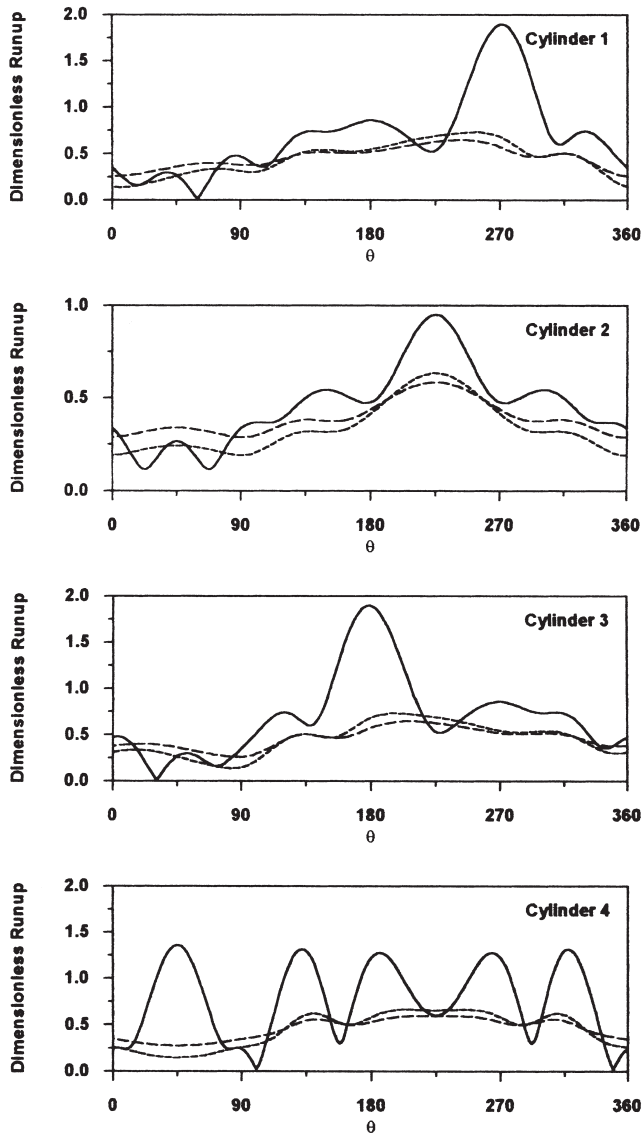


Fig. 12. Dimensionless run-up on outer wall of each cylinder of four-cylinder array for $s/a = 4$, $\beta = 45^\circ$ and $ka = \pi$. Notations: — $G_0 = 0$; --- $G_0 = 1$; -.- $G_0 = 2$.

$= 4$, an incident wave angle $\beta = 45^\circ$, porosity parameters $G_0 = 0, 1, 2$, for diffraction parameters $ka = \pi/2$ and π . It can be seen that the porosity decreases the magnitude of the maximum run-up on the outer walls of the cylinders, and makes the run-up relatively insensitive to location on the cylinder. Furthermore, increasing the porosity parameter G_0 from 1 to 2 does not appear to have a significant influence on the wave run-up.

The influence of porosity on the magnitude of the free surface elevation on, and in the vicinity of a four cylinder array is presented in Figs. 14–17 for $d/a = 5$, $s/a = 4, 8$, $\beta = 0^\circ, 45^\circ$, and $ka = \pi/2$. Each figure shows the results for $G_0 = 0$

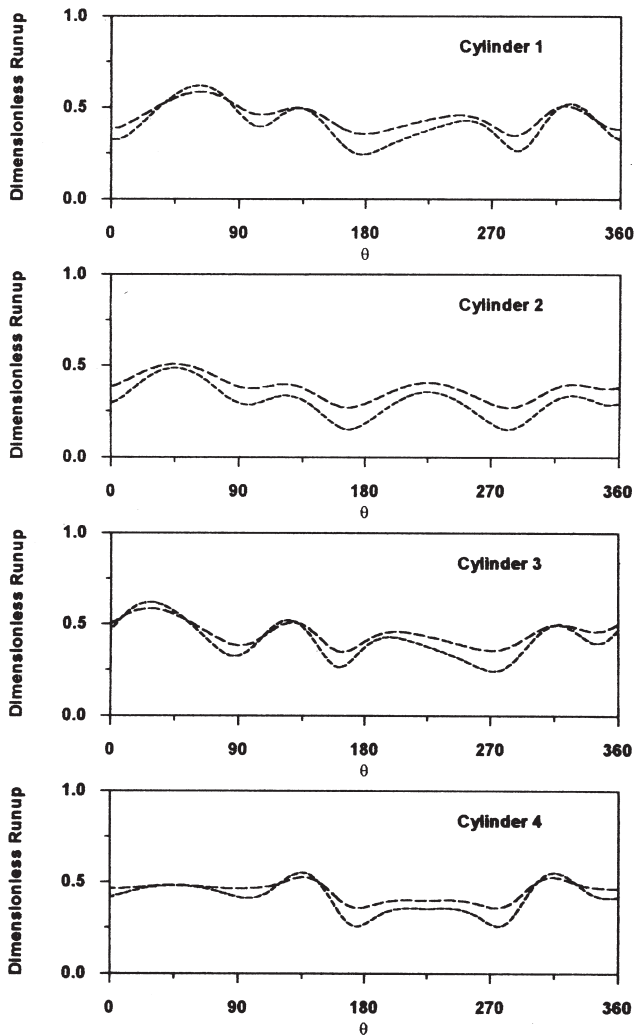


Fig. 13. Dimensionless run-up on inner wall of each cylinder of four-cylinder array for $s/a = 4$, $\beta = 45^\circ$ and $ka = \pi$. Notations: — $G_0 = 0$; - - - $G_0 = 1$; - · - · $G_0 = 2$.

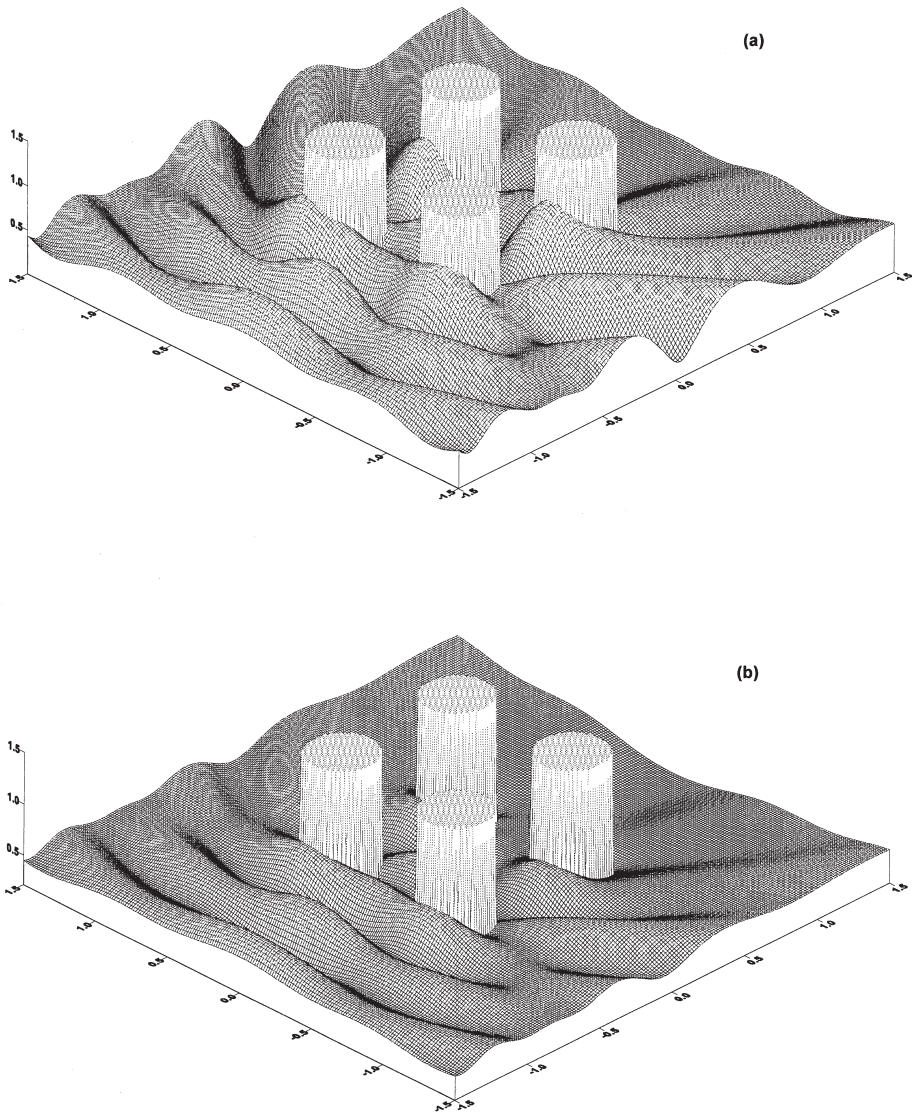


Fig. 14. Free surface elevations for the four-cylinder array for $d/a = 5$, $s/a = 4$, $ka = \pi/2$ and $\beta = 0^\circ$. Notations: (a) $G_0 = 0$; (b) $G_0 = 1$.

(impermeable) and $G_0 = 1$. The figures clearly show the diffraction of the incident wave field by the cylinders, and demonstrate the dramatic effect that the porosity of these cylinders may have on the diffracted wave field especially at the smaller relative spacing, $s/a = 4$.

Figs. 18–20 represent the magnitude of free surface elevation for $s/a = 4$, $d/a = 5$, $G_0 = 0, 1$, incident wave $ka = \pi/2$, and $\beta = 0^\circ, 45^\circ$ and 90° for the case of a

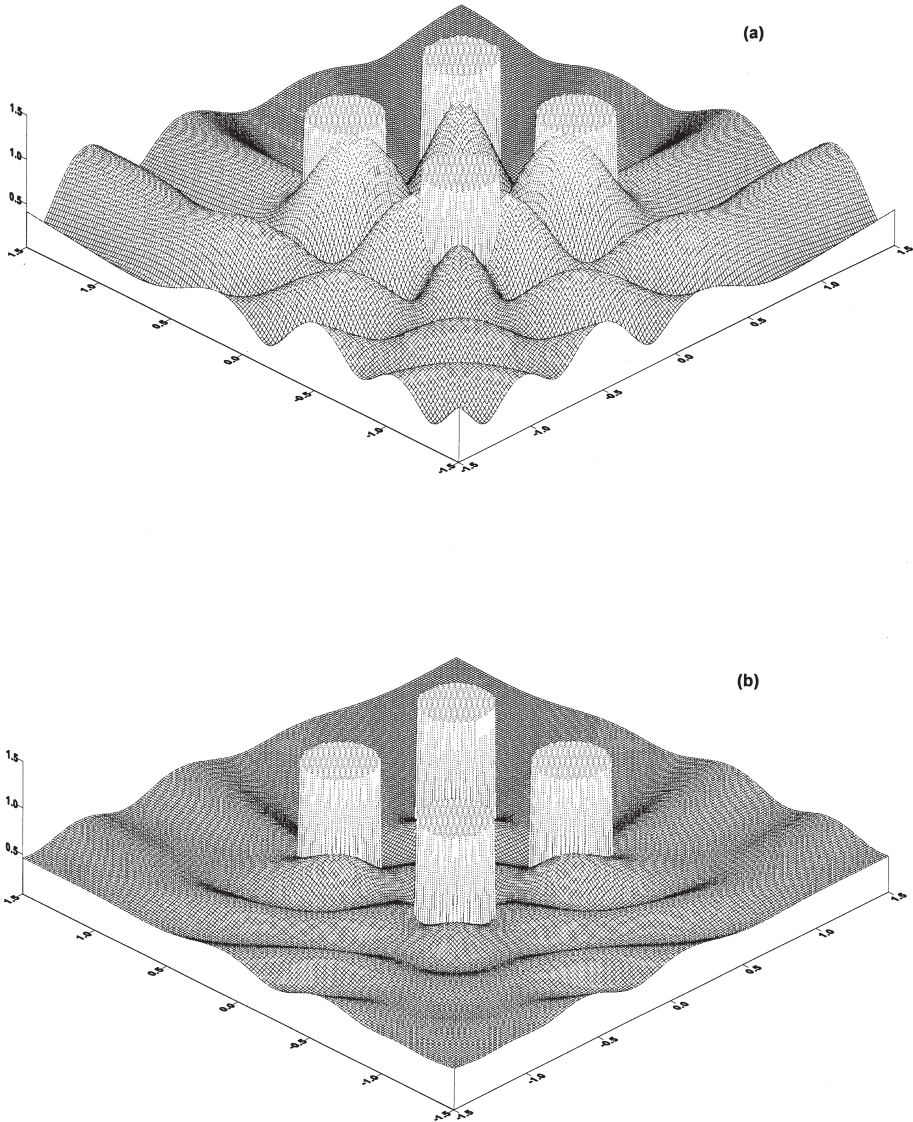


Fig. 15. Free surface elevations for the four-cylinder array for $d/a = 5$, $s/a = 4$, $ka = \pi/2$ and $\beta = 45^\circ$. Notations: (a) $G_0 = 0$; (b) $G_0 = 1$.

six cylinder array, arranged as shown in Fig. 2(b). Again, the diffraction of the incident wave field by the cylinders is shown, together with the influence of the cylinders' porosity on the diffracted wave field. From a practical viewpoint, these figures also highlight the possibility of utilizing a row of porous cylinders as an

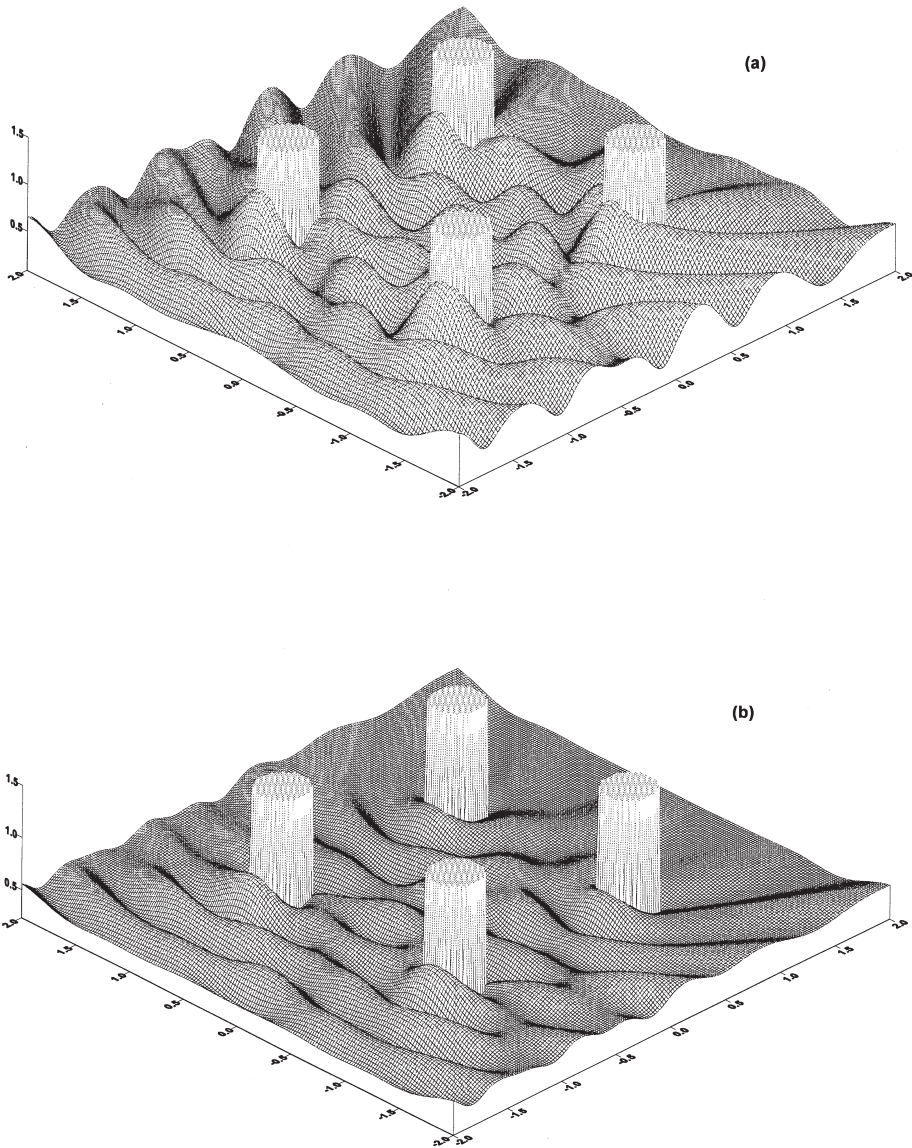


Fig. 16. Free surface elevations for the four-cylinder array for $d/a = 5$, $s/a = 8$, $ka = \pi/2$ and $\beta = 0^\circ$. Notations: (a) $G_0 = 0$; (b) $G_0 = 1$.

offshore breakwater, where their superiority over an array of impermeable cylinders is clearly demonstrated, especially for non-normal wave incidence (Fig. 19).

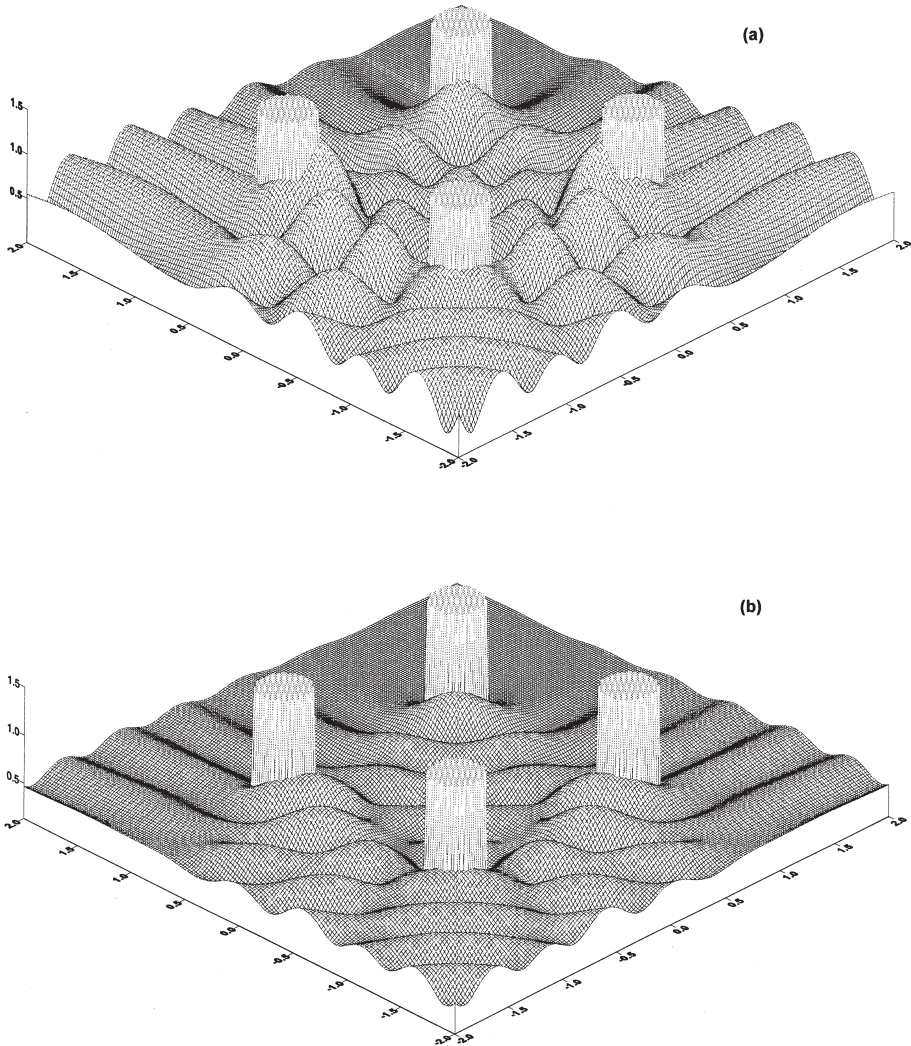


Fig. 17. Free surface elevations for the four-cylinder array for $d/a = 5$, $s/a = 8$, $ka = \pi/2$ and $\beta = 45^\circ$. Notations: (a) $G_0 = 0$; (b) $G_0 = 1$.

5. Conclusions

The interaction of water waves with arrays of bottom-mounted, surface-piercing porous circular cylinders has been investigated theoretically. Under the assumptions of potential flow and linear wave theory, a semi-analytical solution has been obtained by an eigenfunction expansion approach. Analytical expressions have been developed for the wave motion in the exterior and all interior fluid regions. Numerical results

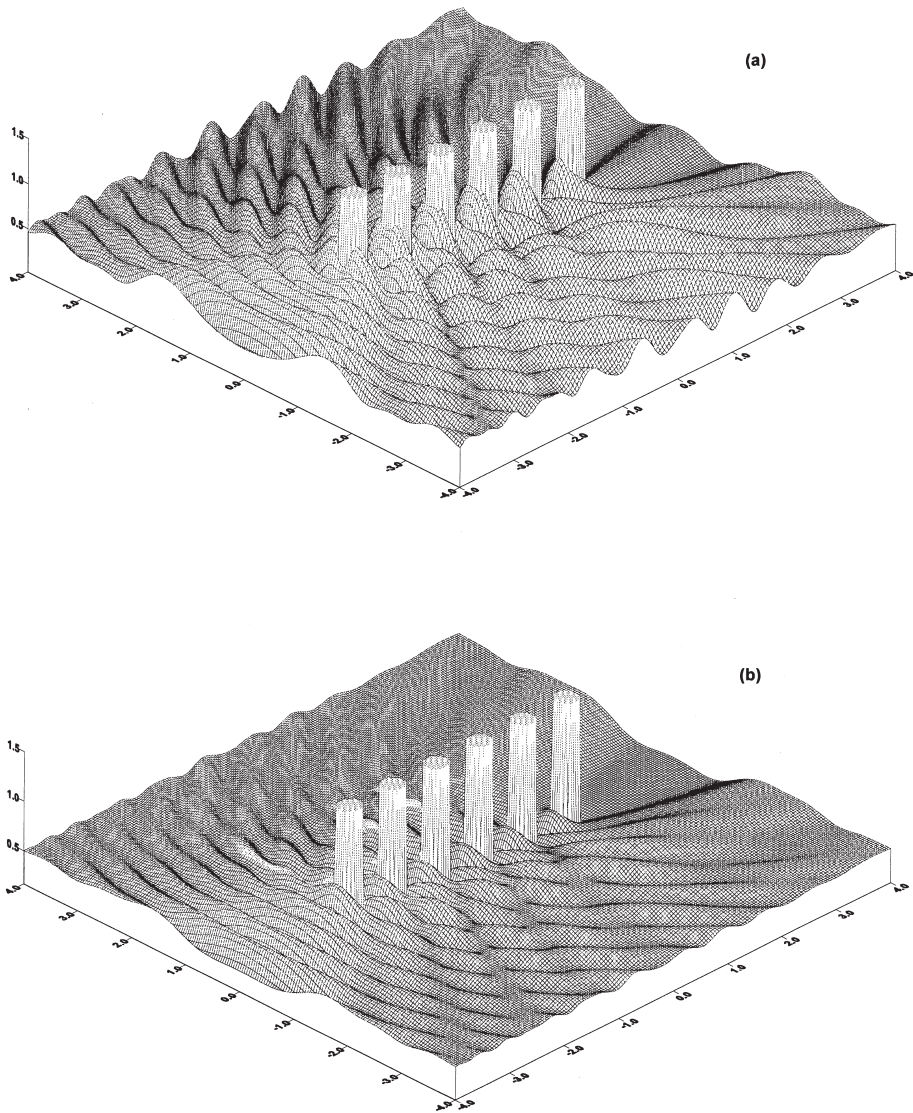


Fig. 18. Free surface elevations for the six-cylinder array for $d/a = 5$, $s/a = 4$, $ka = \pi/2$ and $\beta = 0^\circ$. Notations: (a) $G_0 = 0$; (b) $G_0 = 1$.

have been presented which illustrate the effects of various wave and structural parameters on the hydrodynamic loads and the diffracted wave field. It has been found that the porosity of the structures may result in a significant reduction in both the hydrodynamic loads experienced by the cylinders and the associated wave runup.

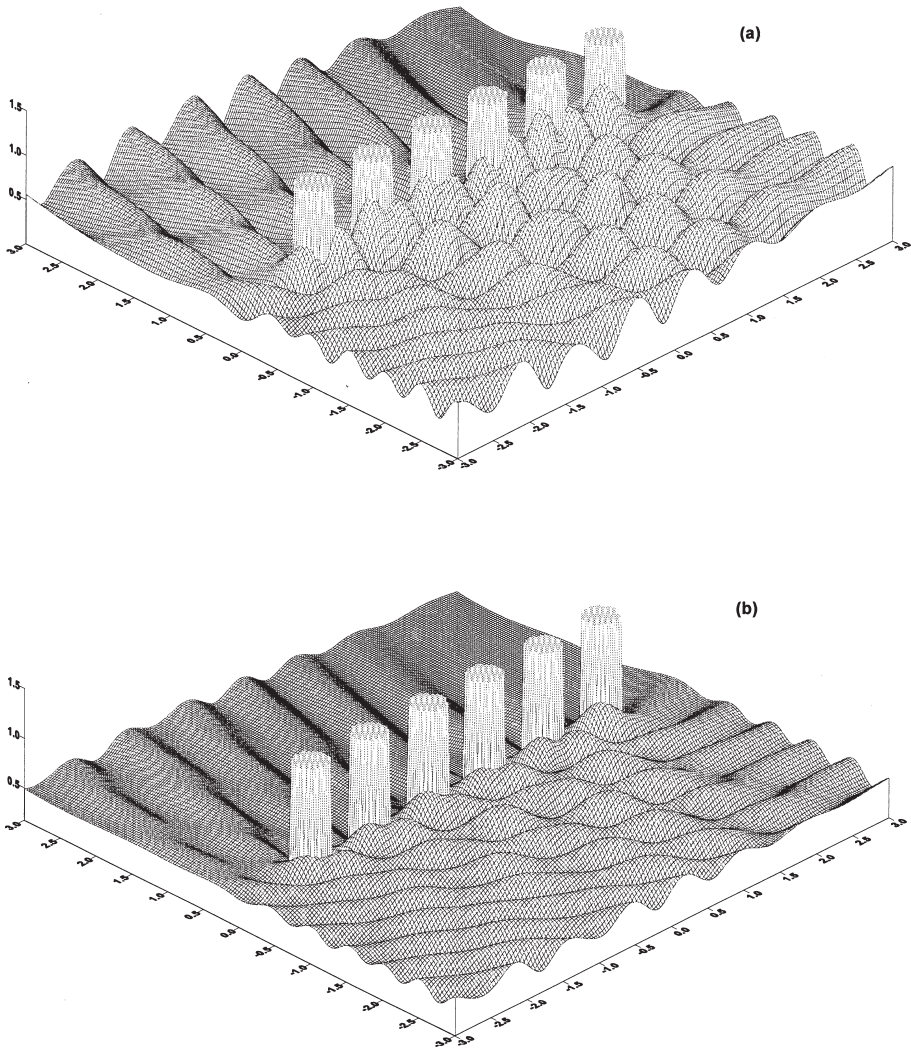


Fig. 19. Free surface elevations for the six-cylinder array for $d/a = 5$, $s/a = 4$, $ka = \pi/2$ and $\beta = 45^\circ$. Notations: (a) $G_0 = 0$; (b) $G_0 = 1$.

Acknowledgements

This work was funded in part by a grant from the Atlantia Corporation of Houston, Texas. This support is gratefully acknowledged.

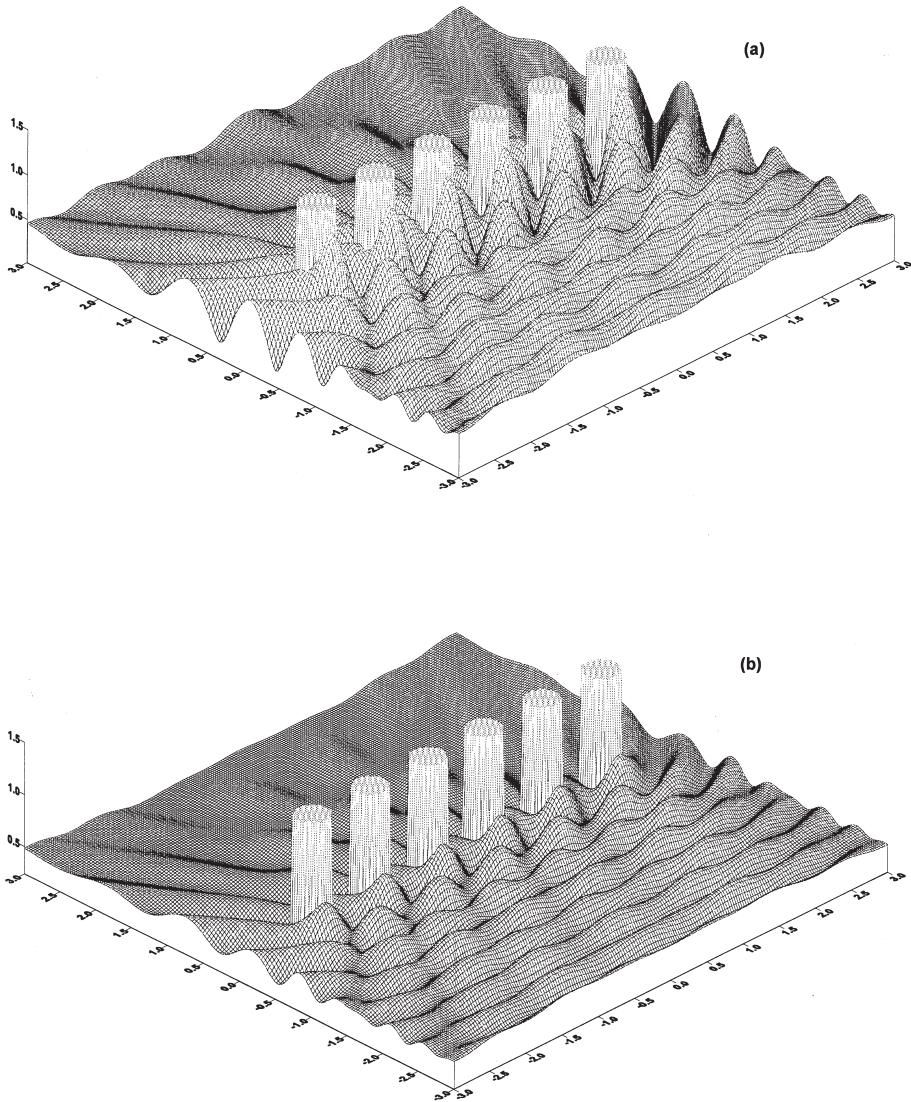


Fig. 20. Free surface elevations for the six-cylinder array for $d/a = 5$, $s/a = 4$, $ka = \pi/2$ and $\beta = 90^\circ$. Notations: (a) $G_0 = 0$; (b) $G_0 = 1$.

References

- Abramowitz, M., Stegun, I.A., 1972. Handbook of Mathematical Functions, Dover Publications, New York.
- Chakrabarti, S.K. 1987. Hydrodynamics of offshore structures. Computational Mechanics Publications, Southampton, UK.

- Darwiche, M.K.D., Williams, A.N., Wang, K.H., 1994. Wave interaction with a semi-porous cylindrical breakwater. *Journal of Waterway, Port, Coastal and Ocean Engineering*, ASCE 120, 382–403.
- Kagemoto, H., Yue, D.K.P., 1986. Interactions among multiple three-dimensional bodies in water waves: an exact algebraic method. *Journal of Fluid Mechanics* 166, 189–209.
- Linton, C.M., Evans, D.V., 1990. The interaction of waves with arrays of vertical circular cylinders. *Journal of Fluid Mechanics* 215, 549–569.
- MacCamy, R.C., Fuchs, R.A., 1954. Wave Forces on Piles: A Diffraction Theory, Tech. Memo No. 69, U.S. Army Corps of Engineers, Beach Erosion Board.
- McIver, P., 1984. Wave forces on arrays of floating bodies. *Journal of Engineering Mathematics* 18, 273–285.
- McIver, P., Evans, D.V., 1984. Approximation of wave forces on cylinder arrays. *Applied Ocean Research* 6, 101–107.
- Spring, B.H., Monkmeyer, P.L., 1974. Interaction of Plane Waves with Vertical Cylinders. Proceedings 14th International Coastal Engineering Conference, Copenhagen, Denmark. 1828–1847.
- Wang, K.H., Ren, X., 1994. Wave interaction with a concentric porous cylinder system. *Ocean Engineering* 21, 343–360.
- Williams, A.N., Demirbilek, Z., 1988. Hydrodynamic interactions in floating cylinder arrays. Part I—Wave scattering. *Ocean Engineering* 15, 549–582.
- Williams, A.N., Abul-Azm, A.G., 1989. Hydrodynamic interactions in floating cylinder arrays. Part II—Wave radiation. *Ocean Engineering* 16, 217–264.
- Williams, A.N., Rangappa, T., 1994. Approximate hydrodynamic analysis of multi-column ocean structures. *Ocean Engineering* 21, 519–573.
- Williams, A.N., Li, W., 1998. Wave interaction with a semi-porous cylindrical breakwater mounted on a storage tank. *Ocean Engineering* 25, 195–219.